Available online at www.sciencedirect.com
ScienceDirect
Trans. Nonferrous Met. Soc. China 24(2014) s106−s111
Transactions of Nonferrous Metals Society of China
www.tnmsc.cn

Microstructure transition from stable to metastable eutectic growth in Ni−25%Al alloy

Zhong-ping QUE[1], Ji-Ho GU[1], Jong-Ho SHIN[2], Je-Hyun LEE[1]

1. Department of Nano and Advanced Materials Engineering, Changwon National University, Changwon, Gyeongnam 641-773, Korea;
2. Doosan Heavy Industries & Construction Co. Ltd., Changwon, Gyeongnam 642-792, Korea

Received 18 June 2013; accepted 14 October 2013

Abstract: The microstructural evolution during directional solidification of the Ni−25%Al (mole fraction) alloy was investigated in the range of growth velocity from 10 to 100 μm/s under a given thermal gradient of 10 K/mm. The solidification microstructures reveal a transition from γ'−β equilibrium eutectic to γ−β metastable eutectic plus β dendrites. A mixed microstructure of γ'−β and γ−β eutectics produced at a growth velocity of 25 μm/s illustrates that the transition occurs during the competitive growth between γ and γ' phases. The growth temperature for each phase was considered to understand the microstructure selection during solidification. The experimental results show that a phase or a microstructure solidifying with the highest temperature under a given growth condition is preferentially selected upon solidification. In addition, both stable eutectic and metastable eutectic are shown to coexist and simultaneously grow in the velocity range between 25 and 60 μm/s due to their similar growth temperatures.
Key words: Ni−Al alloys; directional solidification; intermetallic compound; undercooling; eutectic; growth velocity; microstructure

1 Introduction

In the 1980s and 1990s, much effort has been expended to find out the location of the eutectic and the peritectic points in the binary Ni−Al system [1−5]. Researchers [4−7] confirmed that the eutectic point is located at a higher concentration of Al than the peritectic point and consists of γ' (Ni_3Al) and β (NiAl) as the equilibrium eutectic phases [8].

In directional solidification experiments [9], the quenched solidification interface revealed the presence of a metastable eutectic comprised of γ (Ni-rich) and β phases [5]. Besides, this system was found to possess a peritectic reaction at a composition and a temperature very close to the eutectic reaction. Three different solid phases of γ, γ' and β can be formed from the liquid at the same temperature, albeit the composition and transformation temperature of equilibrium, and metastable eutectics still remain to be controversial. Hence, the solid/liquid interface can preferentially select a microstructure of peritectic or equilibrium eutectic or metastable eutectic during directional solidification.

Ni-based superalloys often contain interdendritic eutectic phases in their as-cast conditions. Non-equilibrium structures formed during solidification should be eliminated through annealing prior to the final heat treatment for the optimal properties of these high-temperature gas turbine materials. Ni_3Al intermetallic compounds exhibit an anomalous dependence of strength with respect to temperature. That is, the mechanical strength increases with increasing temperature at elevated temperatures. Due to the significant role of γ'-Ni_3Al phase in the strengthening of Ni-based superalloys [10−13], it is suggested to further examine the microstructure evolution during the solidification of Ni−Al alloy systems.

The present work was thus carried out to investigate the effect of growth velocity on the microstructure selection during the directional solidification of the Ni−25%Al (atom fraction) alloy at a given thermal gradient. In order to illustrate the microstructure

Foundation item: Project (2011−0030801) supported by the National Research Foundation of Korea
Corresponding author: Je-Hyun LEE; Tel: +82-55-213-3695; Fax: +82-55-261-7017; E-mail: ljh@changwon.ac.kr
DOI: 10.1016/S1003-6326(14)63295-7

selected during freezing, the growth interface temperature for each microstructure was considered a function of growth velocity, and the transition velocity and the transition temperature were analyzed accordingly.

2 Experimental

The phase diagram and thermo-physical parameters for the Ni−Al system are shown in Fig. 1 and Table 1 [8,14,15], respectively. Ni−25%Al (mole fraction) specimens at a hyper-eutectic composition were cast into the water-chilled copper mold to form a 12-inch long ingot with 1-inch diameter. The sample rods of 4.7-mm diameter were prepared from the ingot by elector-discharge machining to fit in a 5-mm diameter alumina tube for directional solidification.

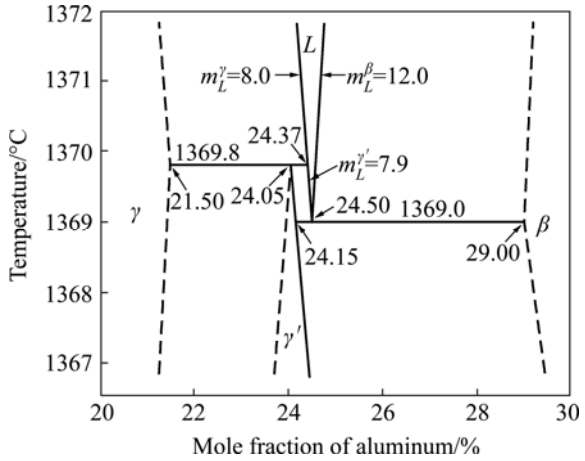

Fig. 1 Phase diagram of binary Ni−Al alloy

Vertical directional solidification experiments were carried out at various velocities ranging from 10 to 100 μm/s under a given thermal gradient, G=10 K/mm. A modified Bridgman type furnace fitted with a water-cooled Cu toroid at the bottom end was moved upwards at controlled stepper motor under an argon pressure of 68.95 kPa. After a directional growth of 40 mm (fraction of solid: f_S=0.7), the alumina tube was dropped into a water bath to preserve the solid microstructure formed at the solid/liquid interface. Here, the same diameter of alumina tubes was used to remove the size effect involved.

The longitudinal and transverse sections of the solidified specimens were polished and etched in Marble reagent (10 g $CuSO_4$+50 mL HCl+50 mL H_2O), and subsequent metallographic observation was conducted using an optical microscope. Volume fraction of each phase and eutectic spacing, λ, were measured on the transverse microstructure for the calculation of the growth interface temperature. In the hyper-eutectic Ni−Al system, the rejected solute is nickel, which is even heavier than aluminum and natural convection can cause the solute to be more segregated radially rather than axially. So, all microstructures were observed in the central part of the specimens to minimize the radial solute segregation by convection.

Table 1 Physical properties of Ni−Al alloy

Phase	Parameter	Value	From Ref.
γ	Gibbs-Thomson coefficient, Γ_γ/(m·K)	1.73×10^{-7}	[8]
	Liquidus slope (vs x(Al)), m_γ/K^{-1}	8×10^{-2}	[14]
	Distribution coefficient, k_γ	0.88	[14]
γ'	Gibbs-Thomson coefficient, $\Gamma_{\gamma'}$/(m·K)	2.71×10^{-7}	[8]
	Liquidus slope (vs x(Al)), $m_{\gamma'}$/K^{-1}	7.9×10^{-2}	[14]
	Distribution coefficient, $k_{\gamma'}$	0.986	[14]
β	Gibbs-Thomson coefficient, Γ_β/(m·K)	1.75×10^{-7}	[8]
	Liquidus slope (vs x(Al)), m_β/K^{-1}	12×10^{-2}	[14]
	Distribution coefficient, k_β	1.184	[14]
$\gamma-\beta$	Eutectic temperature, T/°C	1369.00	[14]
	Eutectic composition (vs x(Al))	24.5	[14]
	Contact angle for γ, θ_γ/(°)	50.4	[8]
	Contact angle for β, θ_β/(°)	6.3	[8]
$\gamma'-\beta$	Eutectic temperature, T/°C	1369.02	[14]
	Eutectic composition (vs x(Al))	24.5	[14]
	Contact angle for γ', $\theta_{\gamma'}$/(°)	26.7	[8]
	Contact angle for β, θ_β/(°)	1.7	[8]

3 Results

In the present work, the metastable $\gamma-\beta$ lamellar eutectic structure was evolved from the stable $\gamma'-\beta$ rod-type eutectic structure with an increase in growth velocity during the directional solidification of the Ni−25%Al (mole fraction) alloy. Figure 2 shows the longitudinal microstructures of the samples grown at velocities between 10 and 100 μm/s. As can be seen from the longitudinal microstructures, the eutectic interface maintains an isothermal condition. Figure 3 shows the transverse microstructures just below 1 mm from the quenched solid/liquid interface. In these figures, γ', β and γ phases are distinguished by their colors: bright γ', black β and gray γ phases. All experimental results on the microstructural features of the solidified Ni−25%Al (mole fraction) alloy specimens are listed in Table 2.

3.1 Stable eutectic structure

The stable eutectic structure composed of γ' cell and β phases on its periphery was observed when a sample

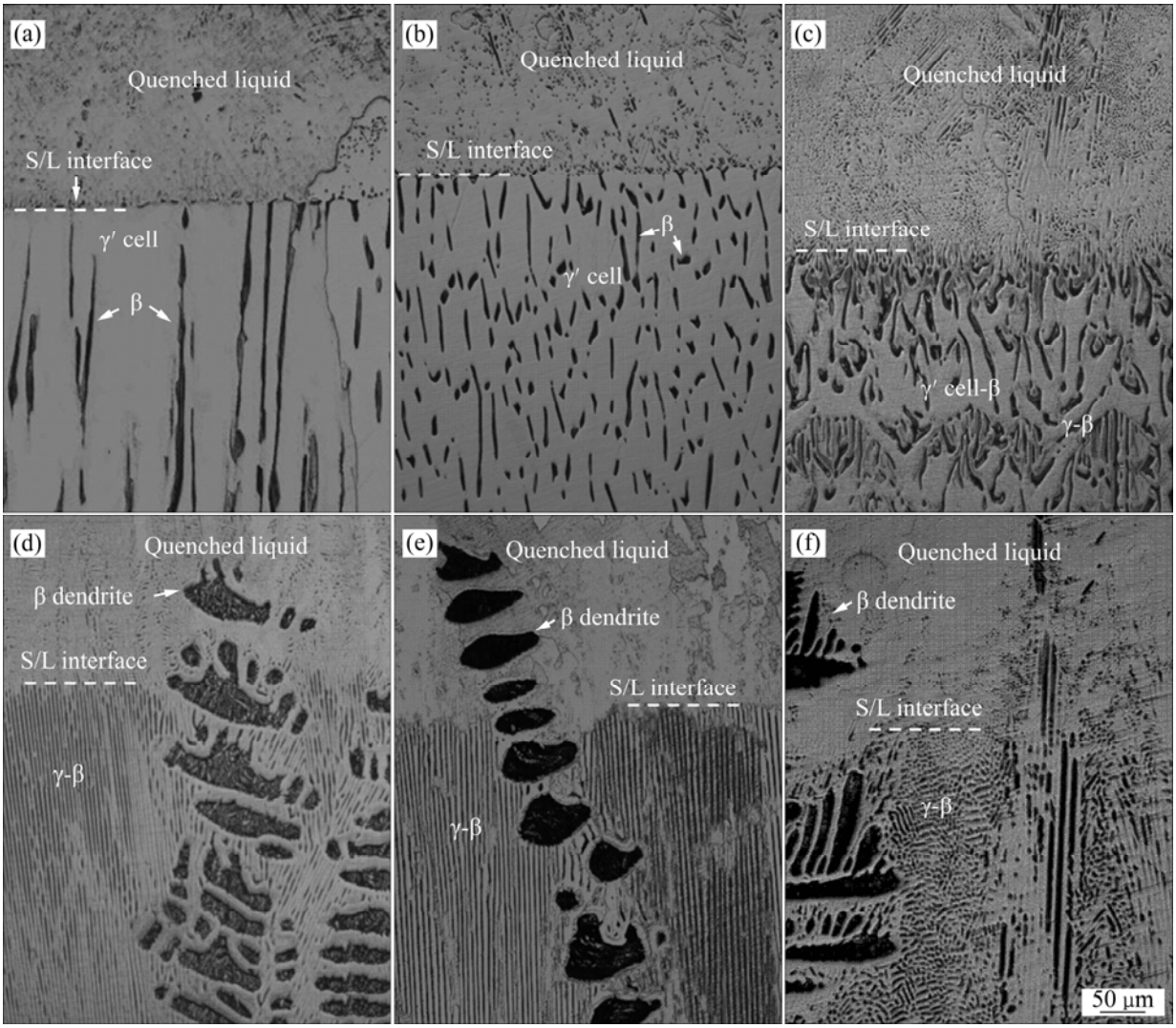

Fig. 2 Longitudinal micrographs in vicinity of solid/liquid interface with different growth velocities: (a) 10 μm/s; (b) 20 μm/s; (c) 25 μm/s; (d) 50 μm/s; (e) 60 μm/s; (f) 100 μm/s

grew at relatively low growth velocities, as shown in Figs. 2 and 3. The regular γ' cell−β structure observed in the sample solidified at 10 μm/s became irregular with increasing growth velocity.

The eutectic spacing is shown to decrease with an increase in the growth velocity, as shown in Figs. 3(a) and (b). When the alloy sample was solidified at 25 μm/s, the metastable γ−β phases were found to grow simultaneously with the stable γ' cell−β structure, as shown in Fig. 2(c) and Fig. 3(c). It seems to be very clear that the increased velocity promotes the nucleation of the metastable γ−β lamellar eutectic and it grows competitively with that stable eutectic. At velocities higher than 25 μm/s, the volume fraction of the irregular γ' cell−β structure decreased with increasing velocity and no irregular eutectic structure was found in the sample grown at 100 μm/s, as shown in Fig. 3(f). It appears that the interface microstructure is determined by the competition between the two eutectic structures. Hence, a mixture of the irregular γ' cell−β and the lamellar γ−β eutectics observed in the sample solidified at 25 μm/s is considered a transient microstructure that demonstrates an evolution from the stable state to the metastable state. It also implies that this kind of mixed structure reflects the concentration changes ahead of the interface with increasing growth velocity and can coexist in a certain velocity range until either structure holds a lead.

Therefore, the microstructure evolution with an increase in growth velocity stems from the increasing concentration of the solute rejected from the interface accordingly. The growth interface temperature correspondingly falls from the growth temperature of the stable γ' cell−β eutectic to that of the metastable γ−β eutectic. In a certain range of velocity, the growth temperatures of the stable eutectic and the metastable eutectic are so analogous that both structures are able to grow concurrently.

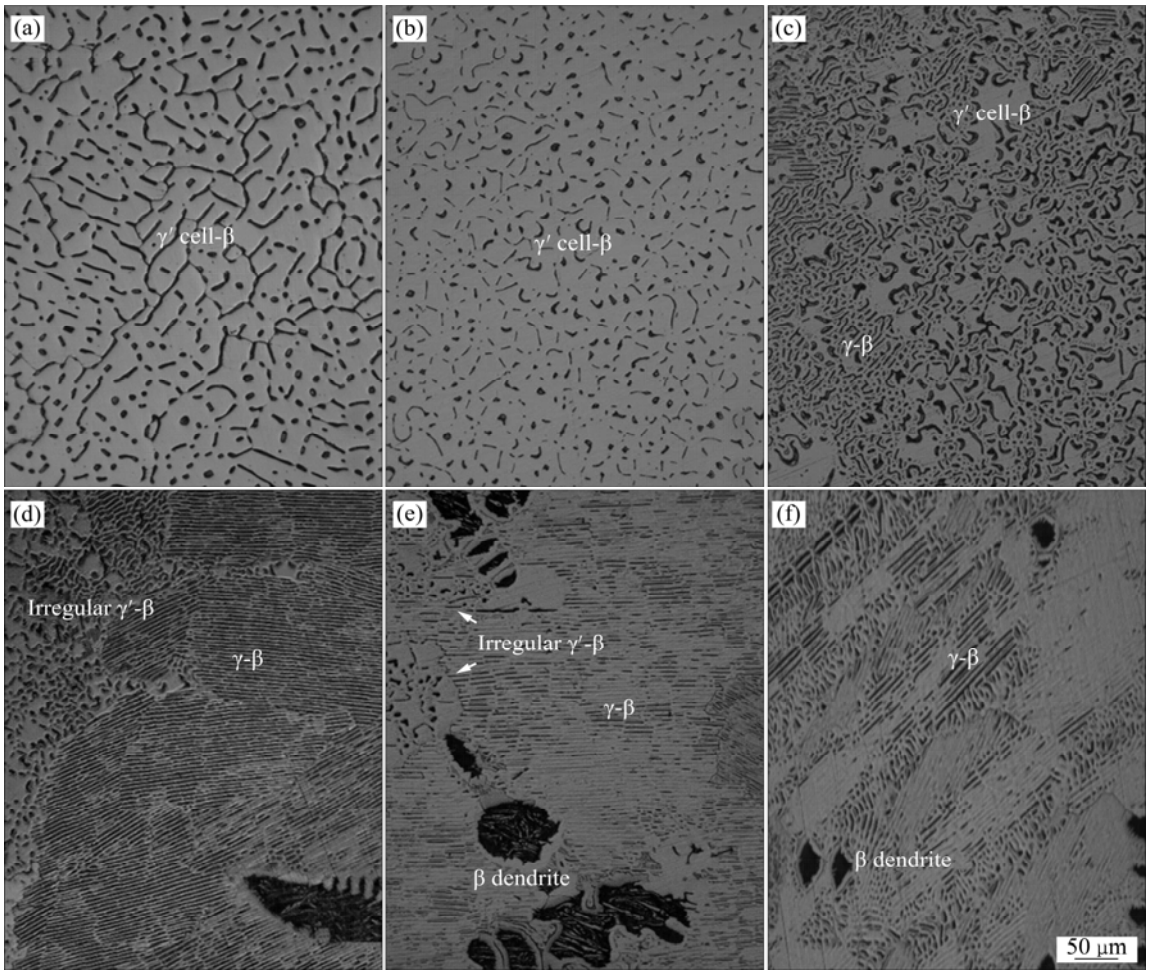

Fig. 3 Transverse microstructures observed right below eutectic interface as a function of growth velocity: (a) 10 μm/s; (b) 20 μm/s; (c) 25 μm/s; (d) 50 μm/s; (e) 60 μm/s; (f) 100 μm/s.

Table 2 Experimental data obtained from directional solidification of Ni−25%Al (mole fraction) alloy

v/(μm·s^{-1})	(G/V)/(K·s·μm^{-2})	f_S	Primary structure	Eutectic structure
10	1×10^{-3}	0.7	(γ' cell−β) eutectic	R (γ'−β) P
20	0.5×10^{-3}	0.7	(γ' cell−β) eutectic	I (γ'−β) P
25	0.4×10^{-3}	0.7	(γ' cell−β)−(γ−β) eutectic	I (γ−β) ME, R (γ'−β)
50	0.2×10^{-3}	0.7	β dendrite	I (γ−β) ME
60	0.16×10^{-3}	0.7	β dendrite	L/I (γ−β) ME
100	0.1×10^{-3}	0.7	β dendrite	Cellular L (γ−β) ME

Note: P—Plane front; L—Lamellar structure; R—Rod-type structure; I—Irregular structure; ME—Metastable eutectic.

3.2 Metastable eutectic structure

With an increment in growth velocity, the β dendritic structure began to form. At the same time, the γ−β metastable eutectic rather than the γ'−β stable eutectic was observed to grow dominantly among the β dendrites. It can be seen from Figs. 2 and 3 that the interdendritic composition decreased sharply with the development of the β dendrites. The metastable eutectic starts to form at a growth velocity of 25 μm/s and at a velocity of 50 μm/s, the fine γ−β lamellar structure and the irregular γ' cell−β structure were observed together in the interdendritic region, suggesting that the interdendritic composition dropped down to the metastable eutectic composition. At a higher velocity, 60 μm/s, a very small amount of the irregular phases were observed in the vicinity of β dendrites. The lamellar γ−β metastable eutectic structure starts to grow cellularly and no irregular eutectic was observed when solidified at 100 μm/s, as shown in Fig. 2(f) and Fig. 3(f). As mentioned above, the irregular eutectic structure represents the growth competition between the stable eutectic and the metastable eutectic and it was demonstrated to be present in a certain velocity range.

4 Discussion

The microstructure evolution presented in Figs. 2

and 3 shows that the interface adopts the eutectic structure corresponding to the minimum undercooling for a given growth condition. The interface morphology can be controlled by the growth conditions such as thermal gradient, growth velocity and alloy composition. In the hyper-eutectic Ni−25%Al (mole fraction) alloy, the increase in growth velocity under a constant thermal gradient led to an increase in solute concentration in liquid ahead of the interface.

The rod-type $\gamma'-\beta$ stable eutectic was observed at 10 μm/s and changed into much less regular shapes at 20 μm/s, as shown in Figs. 3(a) and (b), respectively. The lamellar $\gamma-\beta$ metastable eutectic began to form at 25 μm/s and was shown to take the lead in microstructure at velocities higher than 50 μm/s. A mixed eutectic structures given in Fig. 3(c) consisted of the stable $\gamma'-\beta$ eutectic and the metastable $\gamma-\beta$ eutectic, indicating the microstructure transition. Moreover, this form of irregular structure also explains that the competitive growth between the stable eutectic and the metastable eutectic occurred in the velocity range from 25 to 60 μm/s.

In order to verify the microstructure evolution as a function of growth velocity, the growth interface temperature for each microstructure was considered. The eutectic interface temperature was calculated by the Jackson−Hunt model [16] for the stable rod eutectic and the metastable lamellar eutectic structures, where the volume fraction of the β phase and the spacing in rod and lamellar eutectic structures were measured for each velocity condition, and the minimum spacing in the Jackson−Hunt model was used for calculating the undercooling of rod and lamellar eutectics.

$$T_i(E) = T_{\mathrm{E}} - \Delta T_{\mathrm{E}} = T_{\mathrm{E}} - \left(K_{\mathrm{c}} V \lambda + \frac{K_{\mathrm{r}}}{\lambda} \right) \tag{1}$$

where

$$K_{\mathrm{c}} = mPC_0 / (f_\alpha f_\beta D) \tag{2}$$

$$K_{\mathrm{r}} = 2m\delta(\Gamma_\alpha \sin\theta_\alpha / m_\alpha f_\alpha + \Gamma_\beta \sin\theta_\beta / m_\beta f_\beta) \tag{3}$$

$$m = m_\alpha m_\beta / (m_\alpha + m_\beta) \tag{4}$$

where m_α and m_β are the liquidus slopes of α phase and β phase, respectively; C_0 is the difference in composition between α phase and β phase; f_α and f_β denote the volume fractions of α phase and β phase, respectively; δ is unity for the lamellar growth and it is $2\sqrt{f_\alpha}$ for the rod growth; P is defined:

For lamellar eutectic,

$$P = \sum_{n=1}^{\infty} \frac{1}{(n\pi)^3} \sin^2(n\pi f_\alpha) \tag{5}$$

For rod eutectic,

$$P = 2f_\alpha \sum_{n=1}^{\infty} \frac{1}{(\gamma_n)^3} \frac{J_1^2(\gamma_n f_\alpha)}{J_0^2(\gamma_n)} \tag{6}$$

where J_1 is the Bessel function of first order and γ_n is approximately equal to $n\pi$.

The interface temperature for the single phase β, $T_i(\beta)$, was calculated by the following model [17].

$$T_i(\beta) = T_{\mathrm{L}} - \frac{GD}{V} - \frac{k\Delta T_0 I(P)}{1-(1-k)I(P)} - \frac{2\Gamma}{R} \tag{7}$$

where T_{L} is the liquidus temperature of β phase; ΔT_0 is the freezing range; P is the Péclet number; R is dendrite tip radius; $I(P)$ is the Ivantsov function.

The calculations show that the phase or structure growing at the highest temperature is preferentially selected for a given growth velocity, as constructed in Fig. 4. It can be seen that the stable rod-type eutectic structure grows at the highest temperature below 20 μm/s, whereas the metastable lamellar eutectic grows behind the leading β dendrite above 50 μm/s. In the velocity range between 25 and 60 μm/s, the difference in the interface temperature between the stable eutectic and the metastable eutectic is shown to be very little. Hence, both phases can coexist in a given growth condition, accounting for the mixed eutectic structure formed at the velocity, as shown in Fig. 3. The microstructure evolution observed in this system is closely related to the variation in solute concentration with growth velocity. It is obvious that a kinetically leading phase or a structure can be selected due to the solute concentration varied as a function of growth velocity.

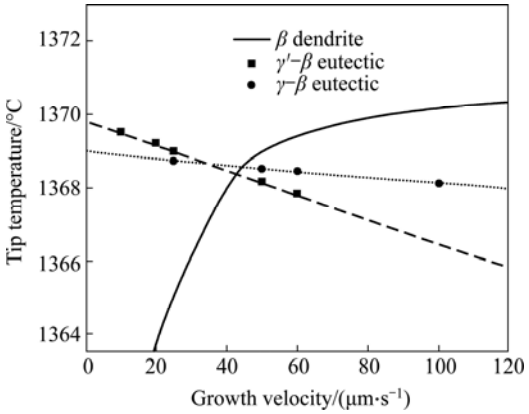

Fig. 4 Interface temperature of stable eutectic, metastable eutectic and β dendrite (The dashed, dotted and solid lines represent the schematic growth temperatures of the stable eutectic, the metastable eutectic and β dendrite, respectively)

5 Conclusions

The directional solidification experiments of the hyper-eutectic Ni−25%Al (mole fraction) alloy are

carried out in the range of growth velocity from 10 μm/s to 100 μm/s under a given thermal gradient of 10 K/mm. The solid/liquid interface microstructures change dynamically from the stable $\gamma'-\beta$ isothermal eutectic structure to the metastable $\gamma-\beta$ lamellar eutectic between β dendrites as a function of growth velocity. A transition from the stable eutectic to the metastable eutectic is observed at a velocity of 25 μm/s. The growth temperature for each phase is considered to understand the microstructure selection during solidification. The experimental results show that a phase or a microstructure solidifying at the highest temperature under a given growth condition can be preferentially selected during solidification. In addition, both stable eutectic and metastable eutectic phases are shown to coexist and to competitively grow in the velocity range between 25 and 60 μm/s due to the strong similarities between their growth interface temperatures. To sum up, the solute rejected from the interface accumulates with an increase in growth velocity, causing the phase or the structure with the highest growth temperature to gain a lead under a given growth condition.

Acknowledgements

This research is also financially supported by Changwon National University in 2011−2013.

References

[1] SINGLETON M F, MURRAY J L, NASH P. Binary alloy phase diagrams [M]. Ohio: American Society for Metals, 1986: 140−143.
[2] SINGLETON M F, MURRAY J L, NASH P. Binary alloy phase diagrams [M]. 2nd ed Ohio: ASM International, 1990: 181−184.
[3] SCHRAMM J. Das teilsystem kobalt-coAl [J]. Zeitschrift für Metallkunde, 1941, 33(10): 347−355.
[4] VERHOEVEN J D, LEE J H, LAABS F C, JONES L L. The phase equilibria of Ni_3Al evaluated by directional solidification and diffusion couple experiments [J]. Journal of Phase Equilibria, 1991, 12(1): 15−23.
[5] LEE J H, VERHOEVEN J D. Metastable eutectic formation in Ni−Al alloys [J]. Journal of Phase Equilibria, 1994, 15(2): 136−146.
[6] HILPERT K, KOBERTZ D, VENUGOPAL V, MILLER M, GERADS H. Phase diagram studies on the Al−Ni system [J]. Zeitschrift für Naturforschung, 1987, 42A: 1327−1332.
[7] BREMER F J, BEYSS M, KARTHAUS E, HELLWIG A, SCHOBER T, WELTER J M, WENZL H. Experimental analysis of the Ni−Al phase diagram [J]. Journal of Crystal Growth, 1988, 87: 185−192.
[8] LEE J H, VERHOEVEN J D. Eutectic formation in the Ni−Al system [J]. Journal of Crystal Growth, 1994, 143: 86−102.
[9] ZHAO Z, QI T, HU P, REN H, LIU L. Alignment and permeability of Al−7Si alloy directional solidification with the application of a pulsed magnetic field [J]. Materials and Manufacturing Processes, 2012, 27(5): 561-566.
[10] HIRANO T, MAWARI T, DEMURA M, ISODA Y. Effect of directional growth-rate on the mechanical properties of Ni_3Al [J]. Materials Science and Engineering A, 1997, 239−240: 324−329.
[11] GOLBERG D, DEMURA M, HIRANO T. Effect of Al-rich off-stoichiometry on the yield stress of binary Ni_3Al single crystals [J]. Acta Materialia, 1998, 46(8): 2695−2703.
[12] LEE K H, WHITE C L. Strain-rate effect on moisture and hydrogen-induced environmental embrittlement of Ni_3Al with and without boron [J]. Scripta Metallurgica et Materialia, 1995, 33(1): 129−137.
[13] CUI Hong-zhi, WEI Na, ZENG Liang-liang, WANG Xiao-bin, TANG Hua-jie. Microstructure and formation mechanism of Ni−Al intermetallic compounds fabricated by reaction synthesis [J]. Transactions of Nonferrous Metals Society of China, 2013, 23(6): 1639−1645.
[14] HUNZIKER O, KURZ W. Directional solidification and phase equilibria in the Ni−Al system [J]. Metallurgical and Materials Transactions A, 1999, 30: 3167−3175.
[15] HUNZIKER O, KURZ W. Solidification microstructure maps in Ni−Al alloys [J]. Acta Materialia, 1997, 45(12): 4981−4992.
[16] JACKSON K A, HUNT J D. Lamellar and rod eutectic growth [J]. Transactions of the Metallurgical Society of AIME, 1966, 236(8): 1129−1142.
[17] TRIVEDI R, KURZ W. Microstructure selection in eutectic alloy systems [C]// STEFANESCU D M, ABBASCHIAN G J, BAYUZIK R J. Solidification Processing of Eutectic Alloys. Warrenddale: TMS, 1988: 3−34.

Ni−25%Al 合金中稳态至亚稳态共晶生长的结构转变

Zhong-ping QUE[1], Ji-Ho GU[1], Jong-Ho SHIN[2], Je-Hyun LEE[1]

1. Department of Nano and Advanced Materials Engineering, Changwon National University, Changwon, Gyeongnam 641-773, Korea;
2. Doosan Heavy Industries & Construction Co. Ltd., Changwon, Gyeongnam 642-792, Korea

摘　要：在 10−100 μm/s 的生长速度范围，热梯度为 10 K/mm 的情况下，研究 Ni−25% Al（摩尔分数）合金定向凝固的微观结构演变规律。凝固组织显示了 $\gamma'-\beta$ 平衡共晶相向 $\gamma-\beta$ 亚稳态共晶加 β 枝晶相的转变。在 25 μm/s 的生长速度时生成的 $\gamma'-\beta$ 和 $\gamma-\beta$ 共晶的混合微观组织表明转变发生在 γ 和 γ'相之间的竞争生长期间。在凝固期间选取微观结构时应考虑各个相的生长温度，试验结果显示在给定生长速度的情况下，在凝固期间，应优先选择在最高温度固化的某个相或微观结构。而且，在 25−60 μm/s 的生长速度范围内，由于稳态和亚稳态共晶具有相似的生长温度，因此可以共存且同时生长。

关键词：Ni−Al 合金；定向凝固；金属间化合物；过冷度；共晶；生长速度；显微组织

(Edited by Lü-xiang DENG)